# Compositional Influence on the Regioregularity and Device Parameters of a Conjugated Statistical Copolymer

**ARTICLE** *in* MACROMOLECULES · FEBRUARY 2013

Impact Factor: 5.8 · DOI: 10.1021/ma302605e



**3 AUTHORS**, INCLUDING:

Dwight Seferos
University of Toronto
**88** PUBLICATIONS **3,716** CITATIONS

Macromolecules

Article

pubs.acs.org/Macromolecules

# Compositional Influence on the Regioregularity and Device Parameters of a Conjugated Statistical Copolymer

Lisa M. Kozycz, Dong Gao, and Dwight S. Seferos*

Lash Miller Chemical Laboratories, Department of Chemistry, University of Toronto, 80 St. George Street, Toronto, Ontario M5S 3H6, Canada

Supporting Information

**ABSTRACT:** We describe a conjugated statistical copolymer, poly(3-hexylthiophene)-*stat*-(3-thiohexylthiophene) (P3HT-*s*-P3THT), with 3-hexylthiophene:3-thiohexylthiophene monomer ratios ranging from 50:50 to 99:1. The copolymer is head-to-tail regioregular in both its hexylthiophene−hexylthiophene and hexylthiophene−thiohexylthiophene linkages, which is not observed in poly(3-thioalkylthiophene) homopolymers. The polymer sequence is random, and the $^1$H NMR spectra have eight distinct aromatic signals that correspond to the eight possible HT−HT regioisomer triads and differ from the spectra expected for the corresponding block or homopolymer systems. When testing the copolymers in bulk heterojunction devices with a fullerene-derivative ($PC_{71}BM$) acceptor, the copolymers have an 11−18% increase in the open-circuit voltage ($V_{oc}$) relative to the P3HT:$PC_{71}BM$ device due to the deeper HOMO level of the 3-thiohexylthiophene unit. This increase is independent of copolymer composition over the 50:50 to 85:15 range and is still observed when there is just one 3-thiohexylthiophene unit in the polymer chain. This shows that statistical copolymers containing as low as 1% of a deep HOMO unit can be used to increase the $V_{oc}$ of the device relative to the parent polymer. All device parameters change in a nonlinear manner as a function of composition, which highlights the distinct properties that can be achieved with conjugated statistical copolymers.

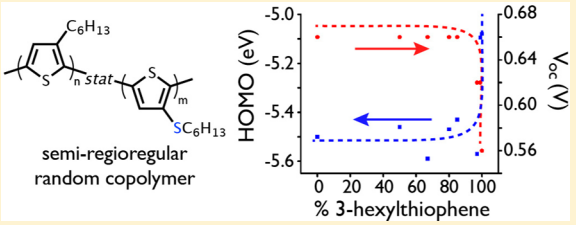


## INTRODUCTION

Historically, the majority of research in polymer solar cells (PSCs) has focused on bulk heterojunction (BHJ) architectures that employ a conjugated homopolymer as the donor material and a fullerene derivative as the acceptor.[1−3] Until recently, poly(3-hexylthiophene) (P3HT) was one of the most successful homopolymers due to its semi-crystalline structure, strong light absorption properties, and high charge carrier mobility.[4] The short-circuit current density ($J_{sc}$) and open-circuit voltage ($V_{oc}$) of P3HT devices are limited, however, due to a wide HOMO−LUMO gap and high HOMO energy level. For these reasons, P3HT device efficiencies have now been surpassed by a new class of copolymers, which typically contain both electron-rich and electron-poor units, resulting in lower HOMO−LUMO gaps and tunable orbital energies.[5−8] Nevertheless, P3HT is still an important material in PSC research because it is easily synthesized and its properties are well understood. Thus, new methods are being developed to copolymerize P3HT with monomers designed to improve device performance, with significant progress having already been made in the area of semi-random P3HT copolymers incorporating small amounts of acceptor monomer to increase the $J_{sc}$.[9−12]

Our group focuses on conjugated diblock copolymers that are comprised of distinct optoelectronic units.[13−15] We recently designed a system to understand how a ternary solar cell functions when two donor materials are covalently bound in a block copolymer arrangement. The polymer was poly(3-thiohexylthiophene)-*block*-(3-hexylthiophene) (P3THT-*b*-P3HT), and when testing P3THT-*b*-P3HT:fullerene solar cells, we found that the lower lying HOMO level of poly(3-thiohexylthiophene) (P3THT) acts to increase the $V_{oc}$ relative to a P3HT:fullerene device fabricated under the same conditions.[16] Although the P3HT block is regioregular, the P3THT block is completely regiorandom due to the lack of Ni catalyst-regioselectivity for 3-thioalkylthiophenes relative to their alkyl counterparts.[17]

When designing new donor materials for PSCs, it is interesting to consider statistical copolymers. Whereas block copolymers can be thought of as two distinct, covalently bound homopolymers, statistical copolymers are a single unique polymer, with properties differing from the block copolymer, the individual homopolymers, or blends of the two. Because the comonomers are randomly incorporated into the chain, statistical copolymers do not undergo phase separation on the 10−20 nm scale, and therefore the solid-state morphology likely differs from the corresponding block copolymer with the same monomer incorporation ratio and chain length. Our group recently studied an equally proportioned poly(3-heptylselenophene)-*stat*-(3-hexylthiophene) system and found

**Received:** December 19, 2012
**Revised:** January 17, 2013
**Published:** January 28, 2013

  

that the optical properties are an average of the two constituent homopolymers, whereas the crystallization and melting behavior are distinct from either homopolymer.[18] Jenekhe and co-workers studied a statistical poly(3-alkylthiophene) (P3AT) with two different linear alkyl chains and found that the crystalline structure and optoelectronic properties were readily tunable by varying the composition.[19] More recently, Thompson and co-workers reported a P3AT copolymer containing linear hexyl and branched ethylhexyl side chains and studied the effect of the composition on device properties in a BHJ solar cell.[20] They found that even small amounts of the ethylhexyl side chain led to a decrease in the HOMO level, resulting in an increase in $V_{oc}$ due to the greater $HOMO_{donor}-LUMO_{acceptor}$ offset. The HOMO level and $V_{oc}$ of the poly(3-hexylthiophene)-*co*-(3-(2-ethylhexyl)thiophene) (P3HT-*co*-P3EHT) devices were composition-dependent, and device performance was optimal for the 75:25 copolymer. This suggests that the incorporation of small amounts of monomer with low-lying HOMO levels is a potential strategy for raising the $V_{oc}$ of a device without lowering the $J_{sc}$ or fill factor (FF). These observations provide motivation to examine the P3HT:P3THT copolymer system as a statistical copolymer.

Herein, we describe the synthesis, characterization, and device performance of the statistical copolymer variant of the P3HT:P3THT system. By statistically incorporating 3-thiohexylthiophene into the chain, we are able to achieve a high $V_{oc}$. By statistically incorporating 3-hexylthiophene into the chain, we improve the regioregularity of the polymer, relative to what can be achieved with a compositionally equivalent diblock copolymer. The goals of this study are to determine (1) the effect of the statistical structure on the mechanism of controlling polymer regioregularity, (2) the minimum amount of 3-thiohexylthiophene incorporation required to increase the $V_{oc}$ of the device to a level that is equivalent to pure P3THT, and (3) how the properties and mechanism of the devices change as a function of statistical incorporation.

## RESULTS AND DISCUSSION

**Synthesis.** The statistical copolymers used in this study were synthesized via Grignard metathesis (GRIM) polymerization using a monomer mixture containing the desired ratio of 2,5-dibromo-3-hexylthiophene and 2,5-dibromo-3-thiohexylthiophene (Scheme 1). A metathesis step was conducted on the

**Scheme 1. Synthesis of Poly(3-hexylthiophene)-*stat*-(3-thiohexylthiophene)**

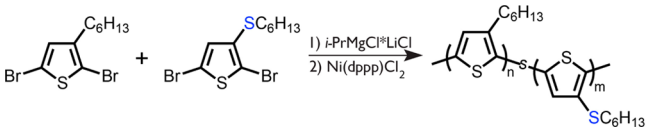


mixture using isopropylmagnesium chloride–lithium chloride complex (Turbo Grignard) at 40 °C for 90 min, followed by treatment with [1,3-bis(diphenylphosphino)propane]nickel(II) chloride [Ni(dppp)$Cl_2$] at 50 °C to initiate and carry out copolymerization. The reactions were terminated after 3 h by treatment with 1 M HCl and precipitated into methanol. The precipitate was then subjected to Soxhlet extraction with methanol, hexanes, and chloroform. The chloroform fraction was further purified by silica gel column chromatography in chloroform.

Polystyrene equivalent molecular weights and polydispersities were determined by gel permeation chromatography (GPC) in 1,2,4-trichlorobenzene at 140 °C (Table 1).

**Table 1. Properties of P3HT-*s*-P3THT Statistical Copolymers**

| monomer ratio A:B[a] | incorporated ratio A:B[b] | $M_n$[c] (kDa) | PDI[c] | P3HT rr[d] (%) | yield[e] (%) |
|---|---|---|---|---|---|
| 95:5 | 99:1 | 17 | 1.8 | 93 | 79 |
| 90:10 | 97:3 | 19 | 1.7 | 92 | 63 |
| 75:25 | 85:15 | 10 | 1.5 | 91 | 12[f] |
| 70:30 | 80:20 | 13 | 1.7 | 84 | 49 |
| 50:50 | 67:33 | 9 | 1.8 | 84 | 29 |
| 40:60 | 50:50 | 9 | 1.5 | 83 | 29 |

[a]3-hexylthiophene:3-thiohexylthiophene monomer feed ratio. [b]3-hexylthiophene:3-thiohexylthiophene ratio in polymer backbone determined by integration of α-methylene peaks at 2.94 and 2.81 ppm. [c]Determined by GPC with polystyrene standards in 1,2,4-trichlorobenzene at 140 °C. [d]Determined by the relative intensity of the α-methylene peaks at 2.58 and 2.81 ppm. [e]Yield of polymer after Soxhlet extraction. [f]Low yield due to experimental error.

Incorporated ratios of 3-hexylthiophene:3-thiohexylthiophene, hereafter known as A:B, were determined by $^1$H NMR by integration of the α-methylene protons on the alkyl side chains (2.81 ppm for A; 2.94 ppm for B). Regioregularity of the AAA linkages was calculated by integrating the α-methylene proton signals at 2.81 ppm (regioregular) and 2.58 ppm (regiorandom). Regioregularity of the other linkages is described in the next section.

A typical quasi-living polymerization with 1 mol % of catalyst should yield polymers with 100 repeat units, which in our synthesis is equivalent to $M_n$ = 16.6 kDa for a 100:0 A:B ratio and $M_n$ = 18.2 kDa for a 50:50 A:B ratio. We note, however, that for polymers with <90% A, the GPC determined $M_n$ is about half the expected value. Additionally, B is incorporated at a 10% lower amount than expected based on the prepolymerization ratio for all copolymers. The yield, as determined by the mass of product from the chloroform fraction before column purification, also decreases with increasing amounts of B. Results are presented for the optimized polymerization conditions (Table 1). We hypothesize that the lower than expected B incorporation can be explained by the enhanced coupling rate of regioregular A–B relative to regiorandom A–B, which prohibits the consumption of all of the B monomer, as well as the presence of some doubly activated 2,5-dichloromagnesio-3-thiohexylthiophene after the metathesis reaction (*vide infra*). It should be noted that the low yield reported for the 75:25 copolymer is due to experimental error and is considered an outlier when considering the aforementioned trend.

**Regioregularity and Randomness.** Significant information about the copolymer sequence and regioregularity is learned by analyzing the aromatic proton resonance signals. For the purpose of this discussion, regioregularity refers to the position of adjacent side chains relative to each other, regardless of the identity of the repeat unit; randomness refers to the sequence of repeat units within the polymer backbone. In our previous study on an equally proportioned P3THT-*b*-P3HT block copolymer we observed that the aromatic $^1$H NMR signals for the 3-hexylthiophene block are a sharp singlet (6.99 ppm), while the aromatic $^1$H NMR signals for the 3-thiohexylthiophene block are a broad multiplet (7.43–7.12


dx.doi.org/10.1021/ma302605e | *Macromolecules* 2013, 46, 613–621

ppm). The differences in peak shape/splitting pattern are attributed to the regioregularity of each block; the P3HT block is regioregular (80%), whereas the P3THT block is regiorandom. Regiorandomness leads to three coupling possibilities: head-to-head (HH), head-to-tail (HT), or tail-to-tail (TT). There are two distinct methodologies for preparing HT regioregular 3-substituted polythiophenes: (1) preparing only one of the two possible activated monomer regioisomers (McCullough method[21]) or (2) preparing both activated monomer regioisomers and employing a polymerization methodology where only one of the two is consumed (Rieke method,[22] GRIM method[23]). When applied to the polymerization of P3ATs, the GRIM methodology uses approach 2. This is due to steric hindrance leading to the selectivity of the Ni catalyst for HT coupling.[24−26] In contrast, when the same conditions are used to polymerize 3-alkoxythiophenes[27] and 3-thioalkylthiophenes,[28] the result is a regiorandom polymer. In these cases, the Ni catalyst is not sterically selective due to the reduced van der Waals radius of O (1.5 Å) or S (1.8 Å) relative to $CH_2$ (2.0 Å).[17]

In the statistical copolymer system under study, we expect linkages between 3-alkylthiophene and 3-thioalkylthiophene units; however, it is unclear whether this would lead to regioregular or regiorandom couplings. It is also important to verify that the structure of the copolymer is indeed random and that unequal reactivity ratios do not result in the formation of a diblock copolymer or two homopolymers. When comparing the $^1$H NMR spectra of the 50:50 P3THT-*b*-P3HT to the 50:50 (incorporated ratio) P3HT-*s*-P3THT (Figure 1), we

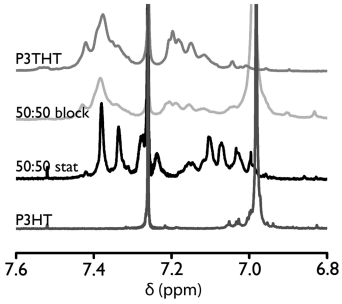


**Figure 1.** $^1$H NMR aromatic resonances of poly(3-thiohexylthiophene), poly(3-hexylthiophene)-*block*-(3-thiohexylthiophene), poly(3-hexylthiophene)-*stat*-(3-thiohexylthiophene), and poly(3-hexylthiophene) (from top to bottom) ($CDCl_3$, 400 MHz).

immediately notice significant differences, which suggest that the statistical copolymer synthesis has resulted in a random sequence. In contrast to the block copolymer spectrum, which contains a sharp singlet and two broad multiplets, the statistical copolymer contains eight major peaks, which appear to be separated into two groups of four. In most P3AT systems, the central proton of each conformational triad (HT−HT, HT−HH, TT−HT, TT−HH) is a distinct proton resonance.[29] In a binary system where each monomer has a distinct resonance, there are eight possible triads (AAA, AAB, BAA, BAB, ABA, ABB, BBA, BBB) and four regioisomers of each triad, resulting in 32 possible resonance signals. From the $^1$H NMR spectrum of the 50:50 statistical copolymer it is clear that there are not 32 equal aromatic peaks. The spectrum appears to be simpler than that. This led us to hypothesize that the eight major peaks correspond to the eight HT−HT conformations and that our system is regioregular (Figure 2). This result was unexpected,

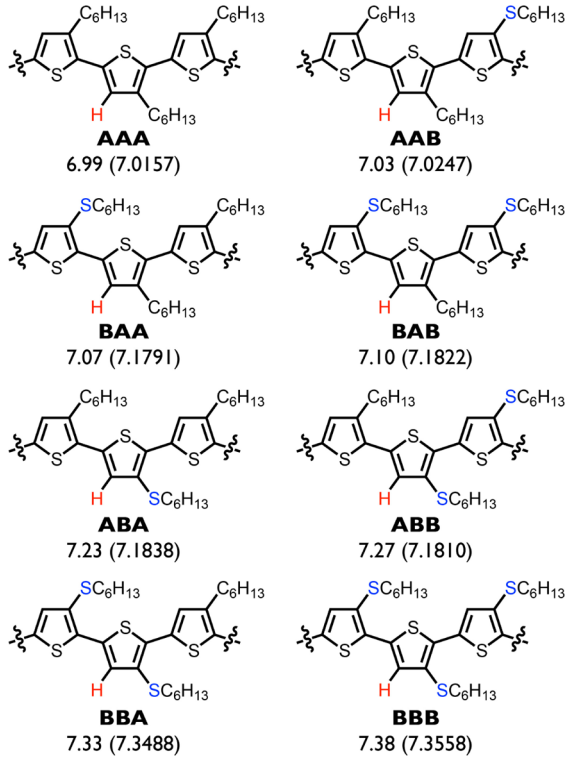


**Figure 2.** Structures of the HT−HT conformational triads for P3HT-*s*-P3THT copolymers with experimental and (predicted) $^1$H NMR resonances for the H-labeled proton (red) (ppm). A = 3-hexylthiophene and B = 3-thiohexylthiophene.

as other HT regioregular AB statistical copolymer systems typically exhibit four aromatic peaks corresponding to AA, AB, BA, and BB (where the signal is from the proton in the 4-position on the second repeat unit).[13,30] In our system, the aromatic resonances seem to be more sensitive to their environment, and the proton shift is dependent on the side chain that is seven bonds away. This sensitivity is consistent with the aromatic spectrum of regiorandom P3THT which spans a 0.41 ppm range, compared to regiorandom P3HT, with its aromatic signals spanning just 0.07 ppm and showing four distinct signals for each of the four conformational triads.[31] The increased sensitivity in P3THT must be due to changes in shielding based on the presence of the sulfur atom, as well as increased rotational freedom around the C−S bond.

To lend further support to these findings we used density functional theory (DFT) calculations to predict the $^1$H NMR spectra of the eight geometry-optimized triads. When the $^1$H NMR spectra of the trimers were predicted using 1-dimensional software, the predicted shifts were identical for each conformation. DFT methods are more accurate for predicting these types of resonances than a 1-dimensional program since they take into account through-space interactions as well as the geometry and 3-dimensional environment of the system. Although the predicted values do not exactly correspond to the experimental ones, we are able to assign experimental values to each HT-HT triad based on the trends of the DFT predictions (Figure 2). There are other minor aromatic peaks in the spectrum, most notably at 7.16 and 7.42 ppm, which are also present in the P3THT spectrum and likely correspond to regiorandom BBB couplings.

Assuming equal reactivity ratios of the A and B monomers, we expect the probability of each of the eight triads to be


dx.doi.org/10.1021/ma302605e | *Macromolecules* 2013, 46, 613−621

identical for the 50:50 statistical copolymer, and therefore the area under each of the eight peaks should be equal. Upon integration of the peaks, we find this to be true, within error. We can use this technique to predict the intensities of the peaks for all A:B ratios and compare the probabilities with the experimental values to further confirm that the eight peaks correspond to the eight HT−HT conformations. When increasing the amount of A, we observe the gradual disappearance of the downfield B shifts and enhancement of the upfield A shifts (Figure 3, left). At 97:3 and 99:1 A:B

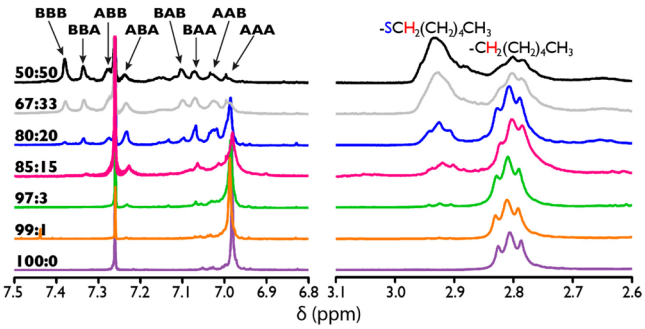


**Figure 3.** $^1$H NMR spectra of P3HT-*s*-P3THT copolymers with distinct aromatic shifts for each HT−HT conformation (left) and each $\alpha$-methylene proton (right). A = 3-hexylthiophene, B = 3-thiohexylthiophene, and H (red) is the proton of interest ($CDCl_3$, 400 MHz).

incorporation ratios, we observe only the two most probable peaks, corresponding to ABA and AAA conformations. The same trend occurs with the $\alpha$-methylene peaks of the side chains (Figure 3, right). The 3-thiohexyl peak at 2.94 ppm decreases with increasing A content. When comparing the predicted and experimental percentage of each HT−HT conformation, we observe that the values are in good agreement; however, the B−B linkages are consistently experimentally lower than predicted (Figure 4). This agrees with the lower B incorporations that were calculated from the $\alpha$-methylene peaks and provides further insight into the mechanism.

**Mechanism.** It is well established that the GRIM polymerization method yields regioregular P3ATs and regiorandom poly(3-thioalkylthiophenes) (P3TATs) (Scheme 2). As previously mentioned, the regioselectivity in P3ATs is

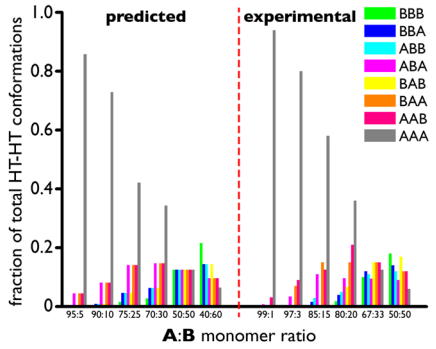


**Figure 4.** Predicted and experimental fractions of each HT−HT conformation for each P3HT-*s*-P3THT composition; A = 3-hexylthiophene and B = 3-thiohexylthiophene. Full structures for each conformation are depicted in Figure 2. Experimental values were obtained by $^1$H NMR integration.

due to the catalyst selectivity for **1**, which is also the more abundant regioisomer. In P3TATs, the catalyst is not selective, and both regioisomers are consumed, although there is some selectivity due to the metathesis step. From the above analysis, we find that the GRIM method leads to regioregular HT−HT couplings between 3-alkylthiophene and 3-thioalkylthiophene monomers, yielding semi-regioregular statistical copolymers when there is less than 50% of the 3-thioalkylthiophene monomer in the polymer chain. This is likely due to a steric effect, where the larger size of the methylene group is significant enough to prevent a HH coupling with **4**. When there is an alkyl group at the 3-position on the active chain end, only HT couplings are permitted, and reaction can only occur with **1** or **3** (Scheme 3A). When the active chain end contains a thioalkyl substituent at the 3-position, HT couplings can occur with **1** and **3**, as well as a HH coupling with **4**, due to decreased steric hindrance (Scheme 3B). This HH coupling results in a third scenario, where there is a thioalkyl group at the 4-position on the active chain end. In this case, couplings are most likely with **1** and **3** due to steric effects as well as the higher abundance of these two monomers. These couplings return the system to one of the first two scenarios, where the substituent is at the 3-position on the active chain end. The HH coupling is the least likely out of the five "probable" couplings outlined in Scheme 3 for copolymers with less than 50% B, since it involves reaction with **4**, the least abundant of the four monomers. These HH−TT trimers likely show up as minor peaks in the $^1$H NMR spectrum, and their low intensities further suggest that this coupling occurs in minor amounts. As the feed of B further decreases, the probability of the B−B couplings also decreases, and hence the overall polymer regioregularity will increase with increasing amounts of A. P3TATs do not have a unique $\alpha$-methylene proton shift for regiorandom couplings, and therefore the regioregularity cannot be quantified.

The fact that HH A−B couplings do not occur helps to explain why the yield, $M_n$, and B incorporation decrease with increasing amounts of B in the monomer mixture. As mentioned above, one of the reasons that the GRIM method prepares regioregular P3ATs is that the metathesis reaction is regioselective. It produces 3-alkyl-2-bromo-5-halomagnesiothiophene (**1**) and 4-alkyl-2-bromo-5-halomagnesiothiophene (**2**) in an 80:20 ratio.[23] Since the Ni catalyst is regioselective for P3ATs, it is likely that 80% of the monomer mixture (**1**) will react to form HT couplings, resulting in a yield and $M_n$ of at least 80% of the theoretical values. The other 20% of monomer (**2**) can theoretically still react, although the reaction is much less likely, and any HH or TT couplings will increase the yield but decrease the regioregularity. In contrast, the metathesis reaction for 3-thiohexylthiophenes is less controlled, and we calculate a 65:35 ratio for 3-thiohexyl-2-bromo-5-chloromagnesiothiophene (**3**) to 4-thiohexyl-2-bromo-5-chloromagnesiothiophene (**4**) after the reaction is quenched with HCl after the metathesis step (see Supporting Information, Figure S8). Using the same logic as applied to the P3AT system, this implies that only 65% of the B monomer should react in a statistical polymerization with A. If the polymerization gets to a point where there are A groups on all the active chain ends and only B monomers left which will result in HH couplings, then no further reaction will occur and the yield, $M_n$, and B incorporation will be lower than expected, as observed in our system.

It is also significant to note that when considering the species present after the activated monomer is quenched with HCl


dx.doi.org/10.1021/ma302605e | *Macromolecules* 2013, 46, 613−621

**Scheme 2. Regioselectivity of the Metathesis Step and Subsequent Polymerization for P3ATs (top), P3TATs (middle), and P3AT-*s*-P3TATs (bottom) under GRIM Conditions**[a]

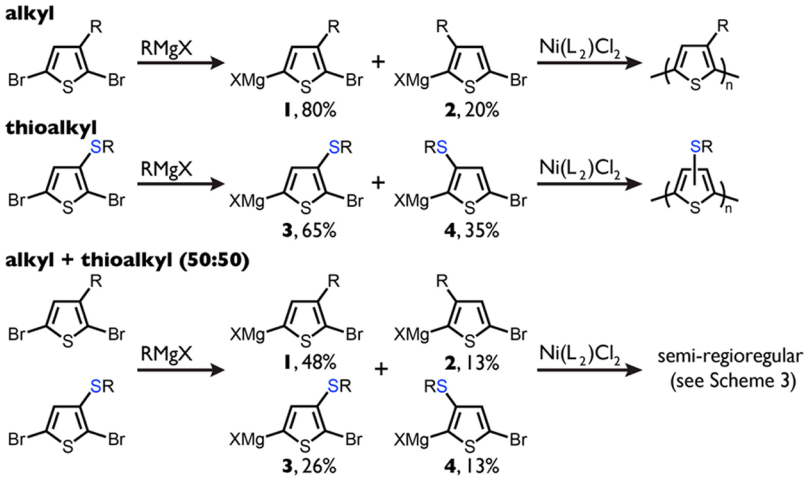


[a]Monomer abundances were obtained by a Grignard quenching experiment. Doubly activated species (see text for details) are excluded for clarity.

**Scheme 3. Probable Couplings for P3AT-*s*-P3TATs When the Active Chain End Is (A) Alkylthiophene or (B) Thioalkylthiophene**

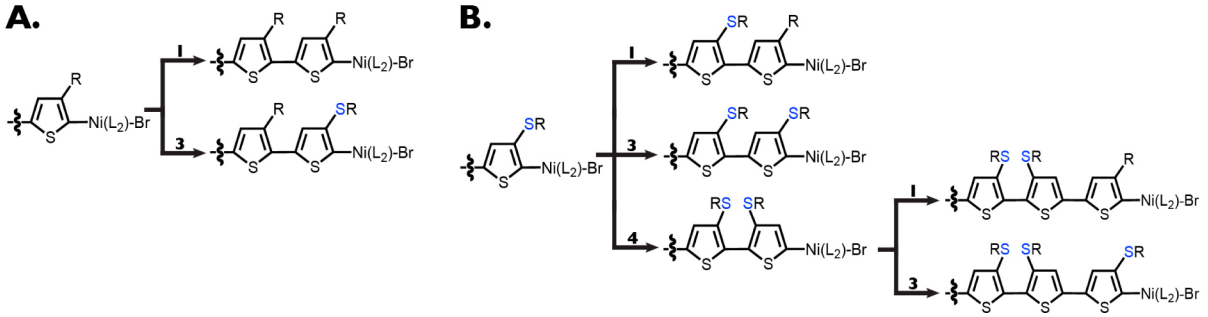


(Figure S8), there is about 10% 3-thiohexylthiophene present in the mixture. This is likely formed due to the presence of excess Grignard reagent which reacts with both bromines of the 2,5-dibromo-3-thiohexylthiophene starting material. Interestingly, only B undergoes this double activation, and we do not observe 3-hexylthiophene in the mixture. Since B appears to be more reactive toward Grignard reagents than A, this provides a second explanation as to why the incorporation of B is consistently lower than expected.

**Absorbance Spectroscopy.** Another method used to evaluate the regioregularity of the copolymers is solid-state absorption spectroscopy. When comparing the 50:50 P3HT:P3THT block copolymer to the statistical copolymer, we observe a red-shift in absorbance as well as an increase in intensity of the shoulder peaks (Figure S9). A polymer with higher regioregularity is more planar, which extends conjugation along the polymer backbone and leads to the red-shifted absorbance. Furthermore, a more planar backbone allows for a greater degree of $\pi-\pi$ stacking, and increased intermolecular vibronic transitions, leading to the more intense shoulder peak at ~610 nm. Therefore, enhanced regioregularity in the statistical copolymer explains these trends in the optical absorption data.

We were also interested in learning how the A:B ratio affects the optoelectronic properties of the copolymer and determining the minimum amount of B required to have an effect on these properties. We observe a red-shifted solution absorbance spectrum in statistical copolymers that have ≥15% B incorporation (Figure 5, top). Increasing B leads to a further red-shift relative to P3HT. The absorbance of the 97:3 and 99:1 copolymers are identical to P3HT, and therefore these small amounts of B are not significant enough to affect the solution absorbance properties of the copolymer.

The changes in the solid-state absorbance spectra are not as pronounced as in solution, and only the 50:50 copolymer is visibly red-shifted relative to P3HT (Figure 5, bottom). The 50:50 and 67:33 copolymers both exhibit a strong shoulder at ~610 nm, and a weaker one at ~525 nm, suggesting that larger amounts of B change the polymer stacking properties in a way that increases intermolecular interactions.

**Device Characterization.** We previously found that when using an equally proportioned P3THT-*b*-P3HT block copolymer as a donor material in a photovoltaic device with a [6,6]-phenyl-$C_{71}$-butyric acid methyl ester ($PC_{71}BM$) acceptor, the $V_{oc}$ is as high as the $V_{oc}$ of the P3THT:$PC_{71}BM$ binary device (0.66 V). This was the first example of an equally proportioned double donor ternary device with a $V_{oc}$ that is as high as the $V_{oc}$ of the corresponding highest voltage binary device and was a promising result as it showed that a high $V_{oc}$ is obtained even if one of the donor materials has a high-lying HOMO level, such as P3HT. Although the $V_{oc}$ of the 50:50 diblock device is high, the $J_{sc}$ and FF are lower than the binary P3HT:$PC_{71}BM$ device, resulting in a lower overall PCE. We hypothesized that by decreasing the amount of the P3THT component relative to


dx.doi.org/10.1021/ma302605e | *Macromolecules* 2013, 46, 613−621

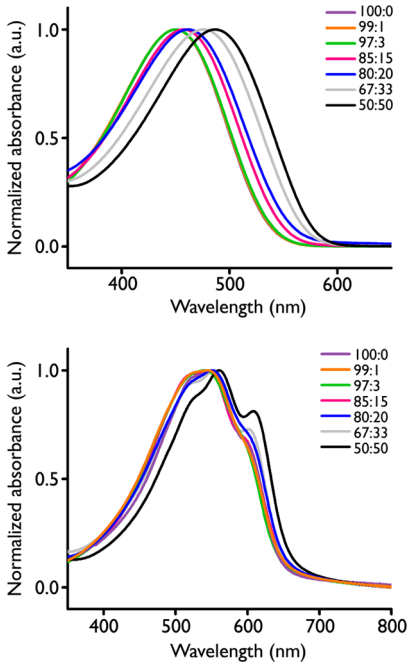


**Figure 5.** Optical absorption spectra of P3HT-*s*-P3THT copolymers (top) in solution (chloroform) and (bottom) thin films (spin-coated from 6 mg/mL chloroform solution at 2500 rpm onto glass substrates), where the polymer is denoted by the line color. A:B = 3-hexylthiophene:3-thiohexylthiophene monomer incorporated into the chain.

P3HT, we would maintain the high $V_{oc}$ while increasing the $J_{sc}$ and FF to values more similar to those obtained for pure P3HT. A second reason for the poor device performance of P3THT-*b*-P3HT is the regiorandomness of the P3THT block. We further hypothesized that by changing the copolymer from a block to a random sequence, we could improve the regioregularity, leading to a more favorable solid-state morphology, similar to that of P3HT. As shown in the previous section, the 50:50 statistical copolymer is more regioregular than the 50:50 diblock, and the regioregularity improves further with more A incorporation.

To test these hypotheses, BHJ solar cells (ITO/PEDOT:PSS/P3HT-*s*-P3THT:$PC_{71}BM$/LiF/Al) were fabricated and characterized (Figure 6). Full device fabrication details can be found in the Experimental Section; *J*–*V* curves and EQE spectra can be found in the Supporting Information (Figures S10 and S11). The results show that as the amount of the A component increases, the $J_{sc}$ and FF increase (nonlinearly) and begin to approach the values measured for pure P3HT (Table 2). Interestingly, the $V_{oc}$ remains higher than the $V_{oc}$ of the pure P3HT device (0.56 V), even for the 99:1 copolymer (0.62 V). The $M_n$ of this polymer is 17 kDa, equivalent to a polymer with about 100 A units and just 1 B unit per chain. For polymers with 15% or more of the B component, the $V_{oc}$ is equivalent to the $V_{oc}$ of the pure P3THT device (0.66 V). Several examples of composition-dependent open-circuit voltages have been reported for statistical copolymers[19,20,32] and ternary systems;[33−36] however, this is the first example of a system where the $V_{oc}$ remains constant and as high as the upper limit voltage of the corresponding binary device over a very large range of compositions (15−100%). Furthermore, no system has ever shown an increase in $V_{oc}$ relative to that of the binary device of the major

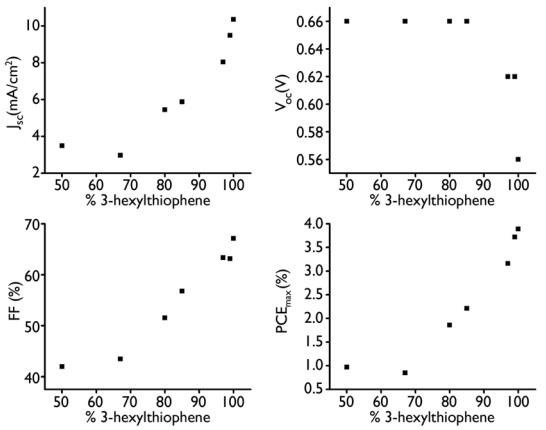


**Figure 6.** Photovoltaic parameters as a function of 3-hexylthiophene content for PSCs fabricated using P3HT-*s*-P3THT:$PC_{71}BM$ and tested under AM 1.5G illumination (100 mW/cm$^2$).

**Table 2. Photovoltaic Properties of P3HT-*s*-P3THT:$PC_{71}BM$ Solar Cells at Different A:B Ratios[a]**

| incorporated ratio A:B | $J_{sc}$ (mA/cm$^2$) | $V_{oc}$ (V) | FF (%) | $PCE_{max}$ (%) | $PCE_{avg}$[d] (%) |
|---|---|---|---|---|---|
| 100:0[b] | 10.36 | 0.56 | 67.10 | 3.89 | 3.67 ± 0.16 |
| 99:1[b] | 9.49 | 0.62 | 63.15 | 3.72 | 3.54 ± 0.15 |
| 97:3[c] | 8.04 | 0.62 | 63.34 | 3.16 | 3.04 ± 0.11 |
| 85:15[c] | 5.88 | 0.66 | 56.80 | 2.21 | 1.87 ± 0.23 |
| 80:20[c] | 5.45 | 0.66 | 51.53 | 1.86 | 1.80 ± 0.04 |
| 67:33[c] | 2.97 | 0.66 | 43.48 | 0.85 | 0.82 ± 0.03 |
| 50:50[b] | 3.50 | 0.66 | 41.97 | 0.97 | 0.79 ± 0.08 |

[a]Devices were spin-coated from 20:20 mg/mL polymer:$PC_{71}BM$ solutions in 1,2-dichlorobenzene at 500 rpm. [b]Active layer was annealed at 100 °C for 5 min. [c]Active layer was vapor annealed at room temperature. [d]Average PCE of eight devices fabricated under identical conditions ± standard deviation.

component, with as low as only 1% of the high $V_{oc}$ component present.

The constant $V_{oc}$ over the 50:50 to 85:15 composition range is consistent with the relatively constant HOMO levels that we measure using cyclic voltammetry (Figure 7). The calculated solid-state HOMO levels are between −5.43 and −5.59 eV for A:B compositions ranging from 50:50 to 97:3. For reference, the calculated solid-state HOMO levels of P3HT and P3THT are −5.08 and −5.46 eV, respectively. This suggests that even

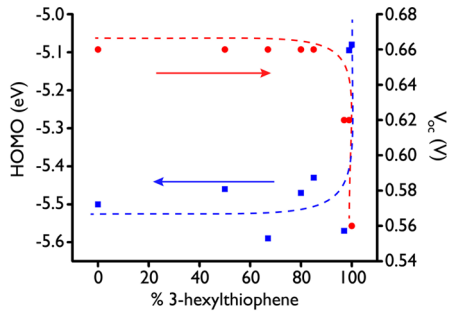


**Figure 7.** HOMO levels of P3HT-*s*-P3THT copolymers in the solid state determined by cyclic voltammetry (blue squares) and $V_{oc}$ of the optimized devices (red circles) as a function of the amount of 3-hexylthiophene monomer in the polymer backbone. The dashed lines are a guide for the eye, and the arrows indicate the appropriate axis.


dx.doi.org/10.1021/ma302605e | *Macromolecules* 2013, 46, 613−621

3% incorporation of the thiohexyl unit is sufficient to lower the HOMO to the same value as the pure P3THT homopolymer. Even though the 99:1 copolymer has a similar HOMO level to pure P3HT, it still results in a device with a higher $V_{oc}$ (0.62 V), indicating that device $V_{oc}$ may be even more sensitive to composition than electrochemistry. Although the LUMO levels were not calculated, we can conclude that they must also be lower in the more B-rich copolymers due to their red-shifted absorbance spectra (Figure 5).

The other three device parameters ($J_{sc}$, FF, and PCE) are composition-dependent over the entire composition range and increase with increasing A content. This increase, however, is nonlinear, and at higher A contents, the increase in all three device parameters is much more pronounced. The difference between the 50:50 and 67:33 devices is almost negligible, and in fact the $J_{sc}$ and PCE slightly decrease with the 17% increase in A, suggesting that device parameters are more sensitive to smaller "defects" in the mainly P3HT backbone, rather than compositional changes in a largely random copolymer. The best PCE for the poly(3-butylthiophene)-*co*-(3-octylthiophene) system was observed in the 50:50 system; however, that polymer did not display a compositional dependence on device parameters.[19] The enhanced performance of the equally proportioned copolymer was attributed to optimal phase separation between the polymer and fullerene phases. In contrast, the P3HT-*co*-P3EHT polymer displayed a quasi-linear increase in $V_{oc}$ with increasing 3-ethylhexylthiophene content and a drastic decrease in $J_{sc}$, FF, and PCE going from a 75:25 to 50:50 3-hexylthiophene:3-ethylhexylthiophene content.[20] The $J_{sc}$, FF, and PCE for the 90:10 device were lower than those for 100:0 and 75:25. Overall, the effect of statistical copolymer composition on device parameters is still not fully understood and seems to differ largely among the various systems.

In this study, the device performance of the 50:50 statistical copolymer ($PCE_{max}$ = 0.97%) is comparable to that of the 50:50 diblock ($PCE_{max}$ = 1.05%), with a slight improvement in the PCE of the diblock due to a higher $J_{sc}$ (statistical: 3.50 mA/cm$^2$; block: 3.83 mA/cm$^2$). This suggests that the improved regioregularity and random copolymer sequence do not lead to an improved device performance in the equally proportioned system, and therefore we can conclude that it is the composition of the thiohexyl-containing copolymers that has the greatest effect on the device performance.

## CONCLUSION

Poly(3-hexylthiophene)-*stat*-(3-thiohexylthiophene) has been synthesized by Grignard metathesis polymerization, characterized, and used as a donor material with $PC_{71}BM$ in a bulk heterojunction solar cell. The statistical copolymer is more regioregular than the corresponding block copolymer due to an increased selectivity for HT couplings between 3-alkylthiophene and 3-thioalkylthiophene units. The percentage of each conformational triad, as well as the incorporated ratio of each monomer, was calculated by $^1$H NMR integration. The yield, molecular weight, and 3-thiohexylthiophene incorporation yield decreases with increasing 3-thiohexylthiophene monomer ratio, likely due to the larger amount of the 4-thiohexyl-2-bromo-5-chloromagnesiothiophene, which is unable to react with 3-hexylthiophene active chain ends, as well as the presence of the doubly activated monomer after the metathesis step.

When testing P3HT-*s*-P3THT:$PC_{71}BM$ solar cell devices, we found that the $J_{sc}$ and FF increase nonlinearly with increasing 3-hexylthiophene content and become more sensitive to compositional changes as the copolymers become more P3HT-heavy. The $V_{oc}$ remains constant, and as high as the $V_{oc}$ of a P3THT:$PC_{71}BM$ binary device, over all compositions up to and including 85:15. This differs from all other statistical copolymer and ternary blend systems, which display a relatively constant increase or decrease over the composition range. The $V_{oc}$ of the 97:3 and 99:1 devices has an intermediate value, in between that of the P3HT:$PC_{71}BM$ and P3THT:$PC_{71}BM$ devices, indicating that only a single 3-thiohexyl chain in a polymer with 100 repeat units is required to affect the voltage of the device. The increased $V_{oc}$ can be partially attributed to the lower HOMO level (relative to P3HT), calculated by cyclic voltammetry; however, the $V_{oc}$ appears to be even more sensitive to minor amounts of comonomer than electrochemistry.

Statistical copolymers have the potential to be a powerful tool for fine-tuning composition-dependent device parameters. Furthermore, the one-pot synthesis of statistical copolymers is more straightforward than block copolymer synthesis, and thus we envision that these results will continue to inspire the design of new statistical copolymers which incorporate narrow HOMO−LUMO gap or highly absorbing monomers into well-studied, high efficiency polymer backbones, such as P3HT.

## EXPERIMENTAL SECTION

**General Considerations.** All reagents were used as received unless otherwise noted. 3-Bromothiophene, 2,5-dibromo-3-hexylthiophene, *n*-butyllithium (1.6 M in hexanes), isopropylmagnesium chloride−lithium chloride complex (1.3 M in THF), and [1,3-bis(diphenylphosphino)propane]nickel(II) chloride ($Ni(dppp)Cl_2$) were purchased from Sigma-Aldrich. *N*-Bromosuccinimide was purchased from Acros Organics and recrystallized in water prior to use.

**Instrumentation and Methods.** NMR spectra were recorded on a Varian Mercury 400 spectrometer operating at 400 MHz. Chemical shifts are reported in ppm at ambient temperature. $^1$H chemical shifts are referenced to the residual protonated chloroform peak at 7.26 ppm. Polymer molecular weights were determined with a Viscotek HT-GPC (1,2,4-trichlorobenzene, 140 °C, 1 mL/min flow rate) using Tosoh Bioscience LLC TSK-GEL $GMH_{HR}$-HT mixed-bed columns and narrow molecular weight distribution polystyrene standards. A UV detector was used to detect the eluted polymer with respect to elution volume. Absorption spectra were recorded on a Varian Cary 5000 UV−vis−NIR spectrophotometer. The thin films used for absorbance spectroscopy were spin-coated from solutions in chloroform (6 mg/mL) at 2500 rpm for 30 s onto glass substrates that had been washed with methanol. Electrochemistry was performed with a BASi Epsilon potentiostat. A standard three-electrode cell with a 2 mm Pt button working electrode, a silver wire pseudoreference electrode, and a Pt wire counter electrode was used, with a ferrocene internal standard and a 100 mV/s scan rate. The electrolyte was a 0.1 M solution of tetrabutylammonium hexafluorophosphate ($TBAPF_6$) in acetonitrile. Polymer films were prepared by drop-casting a 7 mg/mL solution of polymer in chloroform onto the working electrode, and the solvent was evaporated in air. HOMO levels were calculated and converted to the vacuum scale using the equation $E_{HOMO} = -(E_{onset\ ox\ vs\ Fc} + 4.8)$ (eV).

**Density Functional Theory Calculations.** Geometry optimizations were performed using the *Gaussian 09* program,[37] employing the Becke three-parameter hybrid functionals Lee−Yang−Parr (B3LYP) level of theory[38,39] and the 6-311G(d) basis set. The hexyl chains were replaced with methyl groups to reduce computation time. Chemical shifts were calculated as the difference of isotropic shielding constants ($\sigma$) with respect to TMS (HF/6-31G(d) GIAO).

**Device Fabrication.** Polymers and $PC_{71}BM$ (American Dye Source) were mixed in 1,2-dichlorobenzene at 1:1 wt ratio (20:20 mg/mL). Solutions were stirred at 50 °C overnight to ensure complete dissolution. Devices were fabricated on commercial indium tin oxide

(ITO) substrates (Colorado Concept Coatings) that had a sheet resistance of ∼10 Ω/□. These substrates were cleaned in aqueous detergent, deionized (DI) water, acetone, and methanol and subsequently treated in an oxygen-plasma cleaner for 5 min. Next, poly(3,4-ethylenedioxythiophene):poly(styrenesulfonate) (PEDOT:PSS) (Clevios P VP AI 4083) was coated onto the substrates at 3000 rpm and annealed in air at 130 °C for 15 min. After annealing, the substrates were transferred into a nitrogen-filled glovebox, where polymer:$PC_{71}BM$ blends were coated at 500 rpm and dried at room temperature in closed Petri dishes. Some polymer:$PC_{71}BM$ blends were further annealed. The annealing conditions were optimized individually for each polymer to optimize device performance. The polymers with 100:0, 99:1, and 50:50 A:B ratios were annealed at 100 °C for 5 min in the glovebox. The polymers with 99:1, 97:3, 85:15, 80:20, and 67:33 A:B ratios were vapor-annealed at room temperature. A 0.8 nm LiF layer and 100 nm Al anode were thermally deposited through a shadow mask at ∼$10^{-6}$ Torr using an Angstrom Engineering Covap II (Kitchener, Ontario, Canada). Device area is 0.07 $cm^2$ as defined by the area of circular Al anode. *I*–*V* characteristics were measured using a Keithley 2400 source meter under simulated AM 1.5 G conditions with a power intensity of 100 mW/$cm^2$. The mismatch of simulator spectrum was calibrated using a Si diode with a KG-5 filter. EQE spectra were recorded and compared with a Si reference cell that is traceable to the National Institute of Standards and Technology. Eight identical devices were measured for each set of conditions, and both the average and maximum PCE are reported in Table 2.

**Synthesis.** *3-Thiohexylthiophene.* Synthesized as previously reported.[40] $^1$H NMR (400 MHz, $CDCl_3$) $\delta$: 7.31 (q, 1H), 7.12 (d of d, 1H), 7.02 (d of d, 1H), 2.84 (t, 2H), 1.66–1.26 (m, 8H), 0.89 (t, 3H).

*2,5-Dibromo-3-thiohexylthiophene.* Synthesized as previously reported.[16] $^1$H NMR (400 MHz, $CDCl_3$) $\delta$: 6.90 (s, 1H), 2.82 (t, 2H), 1.62–1.26 (m, 8H), 0.89 (t, 3H).

*Poly(3-hexylthiophene)-stat-(3-thiohexylthiophene); Representative Procedure for 50:50 Copolymer.* Isopropylmagnesium chloride–lithium chloride complex (1.3 mL, 1.3 M in THF) was added to a solution of 2,5-dibromo-3-hexylthiophene (212 mg, 0.65 mmol) and 2,5-dibromo-3-thiohexylthiophene (367 mg, 1.02 mmol) in 12 mL of dry THF and heated to 40 °C. After 90 min, the solution was transferred to a flask containing Ni(dppp)$Cl_2$ (9.05 mg, 0.0167 mmol) and heated to 50 °C. After 3 h, the reaction mixture was treated with 1 M HCl and precipitated into methanol. The dark purple precipitate was then subjected to Soxhlet extraction with methanol, hexanes, and chloroform. The chloroform fraction was concentrated to afford the crude polymer (91.2 mg, 29% yield), which was further purified by silica gel chromatography. $^1$H NMR (400 MHz, $CDCl_3$) $\delta$: 7.38 (s, 0.25H), 7.34 (s, 0.25H), 7.28 (s, 0.25H), 7.24 (s, 0.25H), 7.10, (s, 0.25H), 7.07 (s, 0.25H), 7.03 (s, 0.25H), 6.99 (s, 0.25H), 2.93 (br, 2H), 2.80 (br, 2H), 1.68–1.30 (m, 16H), 0.89 (br, 6H). GPC: $M_n$ = 9500 g $mol^{-1}$, $M_w$ = 13 400 g $mol^{-1}$, PDI = 1.5. All statistical copolymers were prepared similarly, varying the ratio of each monomer. For clarity, we refer to the A:B incorporation ratio as determined by $^1$H NMR integration when discussing these polymers.

## ■ ASSOCIATED CONTENT

### Ⓢ Supporting Information

$^1$H NMR spectra, GPC and CV traces of P3HT-*stat*-P3THT copolymers, *J*–*V* and EQE curves of P3HT-*stat*-P3THT:$PC_{71}BM$ devices, Grignard quenching experiment, solid-state absorbance spectra of 50:50 block and statistical copolymers, optimized geometry coordinates, and complete citation for ref 37. This material is available free of charge via the Internet at http://pubs.acs.org.

## ■ AUTHOR INFORMATION

### Corresponding Author

*E-mail dseferos@chem.utoronto.ca.

### Notes

The authors declare no competing financial interest.

## ■ ACKNOWLEDGMENTS

This work was supported by the University of Toronto, NSERC, the CFI, and the Ontario Research Fund. D.S.S. is grateful to the Connaught Foundation (Innovation Award), MaRS Innovation (Proof-of-Principle Grant), and DuPont (Young Professor Grant). The authors thank Sean Campbell and Jim Duliban (Angstrom Engineering) for guidance on the evaporation system used in the device evaluation.

## ■ REFERENCES

(1) Coakley, K. M.; McGehee, M. D. *Chem. Mater.* **2004**, *16*, 4533–4542.
(2) Günes, S.; Neugebauer, H.; Sariciftci, N. S. *Chem. Rev.* **2007**, *107*, 1324–1338.
(3) Cheng, Y.-J.; Yang, S.-H.; Hsu, C.-S. *Chem. Rev.* **2009**, *109*, 5868–5923.
(4) Dang, M. T.; Hirsch, L.; Wantz, G. *Adv. Mater.* **2011**, *23*, 3597–3602.
(5) Chen, H.-Y.; Hou, J.; Zhang, S.; Liang, Y.; Yang, G.; Yang, Y.; Yu, L.; Wu, Y.; Li, G. *Nat. Photonics* **2009**, *3*, 649–653.
(6) Chu, T.-Y.; Lu, J.; Beaupré, S.; Zhang, Y.; Pouliot, J.-R.; Wakim, S.; Zhou, J.; Leclerc, M.; Li, Z.; Ding, J.; Tao, Y. *J. Am. Chem. Soc.* **2011**, *133*, 4250–4253.
(7) Amb, C. M.; Chen, S.; Graham, K. R.; Subbiah, J.; Small, C. E.; So, F.; Reynolds, J. R. *J. Am. Chem. Soc.* **2011**, *133*, 10062–10065.
(8) Albrecht, S.; Janietz, S.; Schindler, W.; Frisch, J.; Kurpiers, J.; Kniepert, J.; Inal, S.; Pingel, P.; Fostiropoulos, K.; Koch, N.; Neher, D. *J. Am. Chem. Soc.* **2012**, *134*, 14932–14944.
(9) Burkhart, B.; Khlyabich, P. P.; Cakir Canak, T.; LaJoie, T. W.; Thompson, B. C. *Macromolecules* **2011**, *44*, 1242–1246.
(10) Khlyabich, P. P.; Burkhart, B.; Ng, C. F.; Thompson, B. C. *Macromolecules* **2011**, *44*, 5079–5084.
(11) Burkhart, B.; Khlyabich, P. P.; Thompson, B. C. *ACS Macro Lett.* **2012**, *1*, 660–666.
(12) Burkhart, B.; Khlyabich, P. P.; Thompson, B. C. *J. Photonics Energy* **2012**, *2*, 021002.
(13) Hollinger, J.; Jahnke, A. A.; Coombs, N.; Seferos, D. S. *J. Am. Chem. Soc.* **2010**, *132*, 8546–8547.
(14) Hollinger, J.; DiCarmine, P. M.; Karl, D.; Seferos, D. S. *Macromolecules* **2012**, *45*, 3772–3778.
(15) Gao, D.; Hollinger, J.; Seferos, D. S. *ACS Nano* **2012**, *6*, 7114–7121.
(16) Kozycz, L. M.; Gao, D.; Hollinger, J.; Seferos, D. S. *Macromolecules* **2012**, *45*, 5823–5832.
(17) Vandeleene, S.; Van den Bergh, K.; Verbiest, T.; Koeckelberghs, G. *Macromolecules* **2008**, *41*, 5123–5131.
(18) Hollinger, J.; Sun, J.; Gao, D.; Karl, D.; Seferos, D. S. *Macromol. Rapid Commun.* **2012**, DOI: 10.1002/marc.201200777. Published Online: Jan17, 2013. http://onlinelibrary.wiley.com/doi/10.1002/marc.201200777/full(accessed Jan 17, 2013).
(19) Wu, P.-T.; Ren, G.; Jenekhe, S. A. *Macromolecules* **2010**, *43*, 3306–3313.
(20) Burkhart, B.; Khlyabich, P. P.; Thompson, B. C. *Macromolecules* **2012**, *45*, 3740–3728.
(21) McCullough, R. D.; Lowe, R. D. *J. Chem. Soc., Chem. Commun.* **1992**, 70–72.
(22) Chen, T.-A.; Rieke, R. D. *J. Am. Chem. Soc.* **1992**, *114*, 10087–10088.
(23) Loewe, R. S.; Khersonsky, S. M.; McCullough, R. D. *Adv. Mater.* **1999**, *11*, 250–253.
(24) Loewe, R. S.; Ewbank, P. C.; Liu, J.; Zhai, L.; McCullough, R. D. *Macromolecules* **2001**, *34*, 4324–4333.
(25) Boyd, S. D.; Jen, A. K.-Y.; Luscombe, C. K. *Macromolecules* **2009**, *42*, 9387–9389.

(26) Tkachov, R.; Senkovskyy, V.; Komber, H.; Kiriy, A. *Macromolecules* **2011**, *44*, 2006−2015.
(27) Koeckelberghs, G.; Vangheluwe, M.; Samyn, C.; Persoons, A.; Verbiest, T. *Macromolecules* **2005**, *38*, 5554−5559.
(28) Vandeleene, S.; Van den Bergh, K.; Verbiest, T.; Koeckelberghs, G. *Macromolecules* **2008**, *41*, 5123−5131.
(29) Mao, H.; Xu, B.; Holdcroft, S. *Macromolecules* **1993**, *26*, 1163−1169.
(30) Palermo, E. F.; McNeil, A. J. *Macromolecules* **2012**, *45*, 5948−5955.
(31) Chen, T.-A.; Wu, X.; Rieke, R. D. *J. Am. Chem. Soc.* **1995**, *117*, 233−244.
(32) Campo, B. J.; Bevk, D.; Kesters, J.; Gilot, J.; Bolink, H. J.; Zhao, J.; Bolsée, J.-C.; Oosterbaan, W. D.; Bertho, S.; D'Haen, J.; Manca, J.; Lutsen, L.; Van Assche, G.; Maes, W.; Janssen, R. A. J.; Vanderzande, D. *Org. Electron.* **2013**, *14*, 523−534.
(33) Khlyabich, P. P.; Burkhart, B.; Thompson, B. C. *J. Am. Chem. Soc.* **2011**, *133*, 14534−14537.
(34) Khlyabich, P. P.; Burkhart, B.; Thompson, B. C. *J. Am. Chem. Soc.* **2012**, *134*, 9074−9077.
(35) Yang, L.; Zhou, H.; Price, S. C.; You, W. *J. Am. Chem. Soc.* **2012**, *134*, 5432−5435.
(36) Koppe, M.; Egelhaaf, H.-J.; Dennler, G.; Scharber, M. C.; Brabec, C. J.; Schilinsky, P.; Hoth, C. N. *Adv. Funct. Mater.* **2010**, *20*, 338−346.
(37) Frisch, M. J.; et al. *Gaussian 09, revision A.1*; Gaussian, Inc.: Wallingford, CT, 2009.
(38) Becke, A. D. *J. Chem. Phys.* **1993**, *98*, 5648−5652.
(39) Becke, A. D. *J. Chem. Phys.* **1996**, *104*, 1040−1046.
(40) Huo, L.; Zhou, Y.; Li, Y. *Macromol. Rapid Commun.* **2009**, *30*, 925−931.